

# Phase Coexistence Properties of Polarizable Water Models

Kenji Kiyohara <sup>1</sup>,

Keith E. Gubbins <sup>2</sup> and Athanassios Z. Panagiotopoulos <sup>3</sup>

*School of Chemical Engineering*

*Cornell University, Ithaca, NY 14853-5201, USA*

February 4, 1998

<sup>1</sup>Present address: Osaka National Research Institute, Ikeda, Osaka 563, Japan

<sup>2</sup>Present address: Chemical Engineering Department, North Carolina State University, Box 7905, Raleigh, NC 27695-7905, USA

<sup>3</sup>Author for correspondence. Present address: Institute for Physical Science and Technology and Department of Chemical Engineering, University of Maryland, College Park, MD 20742-2431, USA, E-mail: thanos@ipst.umd.edu

We report the vapor-liquid coexistence densities near the critical point for polarizable water models, determined by a series of grand canonical Monte Carlo simulations with the histogram reweighting method. Previously proposed point charge models rescaled to match the experimental permanent dipole moment in the gas phase were used. Isotropic polarizability was added to account for three-body and higher order interactions in dense phases. The coexistence density, vapor pressure and heat of vaporization of the models were calculated. The models used in this study, including a recently introduced polarizable model that gives good agreement with the experimental structure, do not give quantitative agreement with the experimental coexistence properties. The potential parameters of the models were varied in an attempt to improve agreement with experimental values for the coexistence properties.

# 1 Introduction

Numerous efforts have been made to model water by a simple potential that is suitable for molecular simulations. Rahman and Stillinger's study [1] using the BNS model [2] clarified many dynamical and structural features of liquid water, and since then a number of water models for computer simulations have been proposed. The SPC [3], the SPC/E [4] and the TIP4P [5] models are widely used. These models consist of a Lennard-Jones interaction site and point charges which represent the electron distribution of the water molecule. The total energy of the system is calculated as a summation of Lennard-Jones and Coulomb interactions between point charges. The potential parameters are usually fitted to thermodynamic and structural properties, such as the internal energy, pressure and pair distribution functions at ambient conditions. In this way, many-body interactions in the liquid phase are effectively accounted for in the parameterization. Thus the dipole moment of the TIP4P model is 2.18D and that of the SPC model is 2.27D: both are higher than the value of an isolated water molecule, 1.85D, because the large polarization effect in the liquid phase is accounted for by adjusting the permanent multipole interactions. Therefore, these models do not represent correctly molecular interactions in the vapor phase. In order to model water interactions over a broad range of densities and temperatures, a possible approach is to introduce polarizability in the potential.

Calculation of the phase coexistence properties of some non-polarizable models can be found in the literature. De Pablo and Prausnitz [6] calculated

phase coexistence densities for the TIP4P model and found that the critical temperature for this model is much lower than the experimental value. For the SPC model, the critical temperature is 10% smaller and the critical density is 16% smaller than experiment [7]. The coexistence densities of the SPC/E model [4] shows better agreement with experiment, but the vapor pressure is too low [8, 9, 10]. In the present work, we have studied the effect of explicit inclusion of polarizability in the potential models on the vapor-liquid coexistence properties.

A number of polarizable water models have been proposed. Some models incorporate the polarization effect by having polarizability sites; point dipoles are induced at these sites in response to the electrostatic fields due to the surrounding molecules [11, 12, 13, 14, 15, 16, 17, 18, 19, 20, 21]. Other models introduce fluctuation of charges [22, 23, 24, 25] or intra-molecular degrees of freedom for the atomic sites [26, 27, 28, 29]. We chose to introduce a single polarizability site on a molecule for reasons of simplicity. We calculated the phase coexistence properties near the critical point for four polarizable point charge models: the polarizable TIP4P model (TIP4P/P), the polarizable SPC model (SPC/P), the SCPDP model of Chialvo and Cummings [20], the model of Kozack and Jordan [17] (KJ), and some variations of the polarizable TIP4P model. We used grand canonical Monte Carlo simulations with the histogram reweighting method [30] for our calculations.

## 2 Model

For the polarizable SPC model and the polarizable TIP4P model, the charges of the original models were rescaled, while maintaining the molecular geometry and Lennard-Jones interaction parameters, to give a dipole moment equal to the experimental value in the gas phase, 1.85D. An isotropic point polarizability equal to the experimental value of 0.001444 nm<sup>3</sup> [31] was introduced on the interaction site of the negative charge. Two polarizable literature models were also studied, the Kozack-Jordan (KJ) model [17] and the SCPDP model [20]. The polarizability of the KJ model is also located on the negative charge, and the parameters of the KJ model were obtained by matching the experimental dipole and quadrupole moments and the second virial coefficients in the gas phase. On the other hand, for the SCPDP model, the polarizability is on the Lennard-Jones interaction site, and the authors fitted the potential parameters to reproduce the experimental pressure, internal energy and the structure at ambient conditions. In general, the total interaction of these potential models can be written as [32]

$$U = U_{cc} + U_{cd} + U_{LJ} \quad (1)$$

with

$$U_{cc} = \sum_{i \neq j} \sum_{k_i, l_j} \frac{Q_{k_i} Q_{l_j}}{|\mathbf{r}_{k_i} - \mathbf{r}_{l_j}|} \quad (2)$$

$$U_{cd} = -\frac{1}{2} \sum_i \mathbf{m}_i \cdot \mathbf{E}_i^c \quad (3)$$

$$U_{LJ} = \sum_{i \neq j} 4\epsilon_{LJ} \left[ \left( \frac{\sigma_{LJ}}{|\mathbf{r}_{LJ_i} - \mathbf{r}_{LJ_j}|} \right)^{12} - \left( \frac{\sigma_{LJ}}{|\mathbf{r}_{LJ_i} - \mathbf{r}_{LJ_j}|} \right)^6 \right] \quad (4)$$

where

$$\mathbf{E}_i^c = \sum_{j(\neq i)} \sum_{l_j} Q_{l_j} \nabla \frac{1}{|\mathbf{r}_{p_i} - \mathbf{r}_{l_j}|} \quad (5)$$

$$\mathbf{m}_i = \alpha \cdot \left( \mathbf{E}_i^c + \sum_{j(\neq i)} \nabla \nabla \frac{1}{|\mathbf{r}_{p_i} - \mathbf{r}_{p_j}|} \cdot \mathbf{m}_j \right). \quad (6)$$

$U_{cc}$ ,  $U_{cd}$ , and  $U_{LJ}$  denote the charge-charge interaction, the charge-induced dipole interaction, and the Lennard-Jones interaction, respectively.  $\mathbf{r}_{k_i}$ ,  $\mathbf{r}_{p_i}$ , and  $\mathbf{r}_{LJ_i}$  are the position vectors of the charge site  $k$ , of the polarization point, and of the Lennard-Jones interaction site of molecule  $i$ , respectively;  $Q_{k_i}$  is the charge at site  $k$  on molecule  $i$ ;  $\epsilon_{LJ}$  and  $\sigma_{LJ}$  are the Lennard-Jones interaction parameters;  $\mathbf{m}_i$  is the induced dipole of molecule  $i$ ;  $\alpha$  is the polarizability tensor;  $\mathbf{E}_i^c$  is the local electrostatic field on the polarization point of molecule  $i$  due to charges on other molecules. For the electrostatic interaction, we employed the Ewald sum [33] to account for the long range interaction. The geometry and the parameters of these models are shown in Table 1 together with the parameters of the original TIP4P and the SPC model.

### 3 Simulation details

For determination of vapor-liquid coexistence and calculation of the coexistence properties of the water models, we used grand canonical Monte Carlo (GCMC) simulations together with the histogram reweighting method. In a GCMC simulation, the chemical potential, the volume, and the temperature

are fixed parameters that determine the thermodynamic state. Microstates having a range of values of the number of molecules,  $N$ , and internal energy,  $U$ , are sampled according to the partition function of the ensemble. At each Monte Carlo step, a new microstate is generated by displacement, rotation and creation or destruction of a molecule. We used 25% of the Monte Carlo steps for each of these four types of move. The energy contribution from the polarization effect was calculated by an iterative procedure [34, 35, 19]. The iteration was continued until the energy difference between the successive estimations was less than 0.01% of the energy. To satisfy this criterion, approximately five iterations were necessary for the convergence of energy at each Monte Carlo step. To use the histogram reweighting method, the number of observations of a particular  $N$  and a particular  $U$  value of the system was stored in the form of a histogram during each GCMC simulation [30, 36, 37]. The grid of the histogram for energy per molecule was chosen to be 0.1 kJ/mol. In order to have good sampling of microstates over a wide range of  $N$  and  $U$  values, we performed several simulations with different chemical potentials and temperatures. In each GCMC simulation, the volume of the simulation box was  $(6 \cdot \sigma_{LJ})^3$  and the length of each simulation was either one half or one million steps. The histograms obtained from all the simulations were combined to calculate vapor-liquid coexistence properties, using the method proposed by Ferrenberg and Swendsen [38]. Pressure was calculated using the virial theorem [35] for low density phases, and the pressures at other conditions were extrapolated using the histogram [30, 36, 37]. For the TIP4P/P model, five sets of simulations for each chemical potential

and temperature were performed in order to estimate the approximate uncertainties in simulation results. We used the square root of the variance of the mean of the five sets of values obtained from the five sets of simulations as the error estimate. The theoretical basis and the detailed procedure of calculation of thermodynamic properties and determination of phase coexistence are described elsewhere [30, 36, 37].

## 4 Results

The calculated coexistence densities of the four polarizable models are shown in Table 2 and Figure 1. We estimated the approximate values of the critical temperature and density by fitting the simulation results to the law of rectilinear diameters and a scaling law, assuming that the models obey the Ising exponent ( $\beta = 0.326$ ). The results are summarized in Table 3. The empirical law of rectilinear diameter is known to be violated near critical points [39, 40]. However, our simulation results are not accurate enough to observe the deviation from the law of rectilinear diameters. The estimated critical temperatures of the TIP4P/P, the SPC/P, and the SCPDP model are smaller than experiment by 10%, 15%, and 17%, respectively, and the critical temperatures of the KJ model is 6% larger than the experimental value. The estimated critical densities of these models are within 10% from the experimental value for all the models studied. The vapor pressures of the TIP4P/P, the SPC/P, and the SCPDP model are too high for the range of temperature studied. The vapor pressure of the KJ model is too low, in

accordance with the high critical temperature of the model (see Figure 2). The heat of vaporizations of the models were also calculated, using the data obtained for energy, pressure, and density (see Figure 3). In general, the coexistence densities of the models we used do not show good agreement with experiment [41, 42].

We made some attempts to optimize the potential parameters to fit the coexistence curve to experimental results. Based on the TIP4P/P model, we varied the Lennard-Jones parameters  $\sigma_{LJ}$  and  $\epsilon_{LJ}$ , the position of the negative charge, and the distance between charges. In the first variation, the  $\sigma_{LJ}$  was reduced by 1% and the other parameters were unchanged. In the second, the  $\epsilon_{LJ}$  was reduced by 20% and the other parameters were unchanged. In the third, the position of the negative charge was shifted towards the positive charges on the H-O-H bisector by 0.005nm, keeping other parameters, except charges, unchanged. In the fourth, the distance between the positive and negative charges was reduced by 1% (other parameters, except charges, unchanged). In the third and the fourth variations, the magnitude of charges were scaled so that the dipole moment for each model remained 1.85D. The results are shown in Figure 4. It is found that a small change in the parameters results in large changes in the values of coexistence density and in the location of critical point; for example, a 1% reduction in  $\sigma_{LJ}$  gives about a 10% increase in critical temperature. Interestingly, a smaller  $\epsilon_{LJ}$  results in a more attractive total interaction energy and a higher critical temperature, because it gives a less steeply repulsive part of the interaction at small separations and permits closer proximity of the partial

charges. ( $\epsilon_{LJ}$  affects both the well depth ( $\epsilon_{LJ}$ ) and the steepness of the repulsion ( $4\epsilon_{LJ} \cdot \sigma_{LJ}^{12}$ ) for a fixed  $\sigma_{LJ}$ .)

The polarizable models that we use do not reproduce well the experimental structure of liquid water at ambient conditions. The original KJ model has been reported not to show good ambient structure [17]. Since liquid structure is sensitive to the detail of the short range repulsive interaction, it may be necessary to improve that part of the potential to reproduce both correct coexistence properties and correct ambient structure by the polarizable water models.

## 5 Conclusions

In the course of modeling interaction of water molecules in a broad range of density and temperature, we calculated the vapor-liquid coexistence properties of four polarizable water models, namely polarizable TIP4P, polarizable SPC, SCPDP, and the Kozack and Jordan model, using GCMC simulations with the histogram reweighting method. The models we used in this study do not give a quantitative agreement with the experimental coexistence properties at elevated temperatures. Even the recently proposed polarizable model, the SCPDP model, which reproduces the thermodynamic properties and the structure at ambient conditions fairly well, does not give accurate coexistence properties. Our attempts at re-parameterization of the polarizable TIP4P model show that a small changes in the potential parameters can significantly change the coexistence properties. The models for which parameters

are adjusted to critical constants do not seem to reproduce experimental ambient structure. It may be necessary to improve the short range repulsive part of the potential in order to reproduce both correct phase behavior near the critical point and correct ambient structure. In a different approach, Müller and Gubbins [43] fitted the potential parameters of a model composed of a Lennard-Jones interaction site, a point dipole moment, and four square well interaction sites that mimic the hydrogen bonding, to reproduce the experimental coexistence curve. Unlike the models with a point polarizability, the square well interaction sites represent a deep and localized interaction. The success of the Müller and Gubbins [43] model suggests that describing properly the deep local minima associated with hydrogen bonding may be essential to describing the thermodynamic behavior of water.

## 6 Acknowledgments

The authors would like to thank Prof. Chialvo and Prof. Cummings for providing copies of papers prior to publication. Financial support for this work was provided by the Department of Energy, Office of Basic Energy Sciences and the National Science Foundation. Supercomputing time was provided by the Cornell Theory Center.

## References

- [1] Rahman, A. and Stillinger, F.H., 1971, *J. Chem. Phys.*, **55**, 3336.

- [2] Ben-Naim, A. and Stillinger, F.H., 1972, Aspects of the Statistical Mechanical Theory of Water, in *Structure and Transport Processes in Water and Aqueous Solutions*, Horne, R.A. (Ed.), (New York: Wiley).
- [3] Berendsen, H.J.C., Postma, J.P.M., van Gunsteren, W.F. and Hermans, J., 1981, in *Intermolecular Forces*, Pullmann, B. (Ed.), Reidel, Dordrecht, 331.
- [4] Berendsen, H.J.C., Grigera, J.R. and Straatsma, T.P., 1987, *J. Phys. Chem*, **91**, 6269.
- [5] Jorgensen, W.L., Chandrasekhar, J., Madura, J.D., Impey, R.W. and Klein, M.L., 1983, *J. Chem. Phys.*, **79**, 926.
- [6] De Pablo, J.J. and Prausnitz, J.M., 1989, *Fluid Phase Equilibria*, **53**, 177.
- [7] De Pablo, J.J., Prausnitz, J.M., Strauch, H.J. and Cummings, P.T., 1990, *J. Chem. Phys.*, **93**, 7355.
- [8] Guissani, Y. and Guillot, B., 1993, *J. Chem. Phys.*, **98**, 8221.
- [9] Alejandre, J., Tildesley, D.J. and Chapela, G.A., 1995, *J. Chem. Phys.*, **102**, 4574.
- [10] Vorholz, J., Harismiadis, V.I., and Panagiotopoulos, A.Z., Unpublished results (1996)
- [11] Barnes, P., Finney, J.L., Nicholas, J.D. and Quinn, J.E., 1979, *Nature*, **282**, 459.

- [12] Stillinger, F.H. and David, C.W., 1978, *J. Chem. Phys.*, **69**, 1473.
- [13] Lybrand, T.P. and Kollman, P.A., 1985, *J. Chem. Phys.*, **83**, 2923.
- [14] Rullmann, J.A.C. and van Duijnen, P. Th., 1988, *Molec. Phys.*, **63**, 451.
- [15] Kuwajima, S. and Warshel, A., 1990, *J. Phys. Chem.*, **94**, 460.
- [16] Dang, L.X., 1992, *J. Chem. Phys.*, **97**, 2659.
- [17] Kozack, R.E. and Jordan, P.C., 1992, *J. Chem. Phys.*, **96**, 3120.
- [18] Wallqvist, A. and Berne, B.J., 1993, *J. Phys. Chem.*, **97**, 13841.
- [19] Bernardo, D. N., Ding, Y., Krogh-Jespersen, K. and Levy, R. M., 1994, *J. Phys. Chem.* **98**, 4180.
- [20] Chialvo, A.A. and Cummings, P.T., 1996, *J. Chem. Phys.*, **105**, 8274.
- [21] Blodholt, J., Sampoli, M., Vallauri, R., 1995, *Molec. Phys.*, **86**, 149.
- [22] Sprik, M. and Klein, M.L., 1988, *J. Chem. Phys.*, **89**, 7556.
- [23] Zhu, S.-B., Singh, S. and Robinson, G.W., 1991, *J. Chem. Phys.*, **95**, 2791.
- [24] Rick, S.W., Stuart, S.J. and Berne, B.J., 1994, *J. Chem. Phys.*, **101**, 6141.
- [25] Svishchev, I.M., Kusalik, P.G., Wang, J. and Boyd, R.J., 1996, *J. Chem. Phys.*, **105**, 4742.

- [26] Taukan, K. and Rahman, A., 1985, *Phys. Rev. B*, **31**, 2643.
- [27] Teleman, O., Jönsson, B. and Engström, S., 1987, *Molec. Phys.*, **60**, 193.
- [28] Dang, L.X. and Pettitt, B.M., 1987, *J. Phys. Chem.*, **91**, 3349.
- [29] Zhu, S.-B. and Wong, C.F., *J. Chem. Phys.*, 1993, **98**, 8892.
- [30] Ferrenberg, A.M. and Swendsen, R.H., 1988, *Phys. Rev. Lett.*, **61**, 2635.
- [31] Moelwyn-Hughes, E.A., 1964, *Physical Chemistry*, p. 383 (New York: Macmillan).
- [32] Gray, C.G. and Gubbins, K.E., 1984, *Theory of Molecular Fluids*, (Oxford: Clarendon).
- [33] De Leeuw, S.W., Perram, J.W., and Smith, E.R., 1980, *Proc. R. Soc. Lond. A* **373**, 27.
- [34] Patey, G.N., Torrie, G.M., and Valleau, J.P., 1979, *J. Chem. Phys.*, **71**, 96.
- [35] Vesely, F.J., 1978, *Chem. Phys. Lett.*, **56**, 390.
- [36] Wilding, N.B., 1995, *Phys. Rev. E*, **52**, 602.
- [37] Kiyohara, K., Gubbins, K.E. and Panagiotopoulos, A.Z., 1997, *J. Chem. Phys.*, **106**, 3338.

- [38] Ferrenberg, A.M. and Swendsen, R.H., *Phys. Rev. Lett.*, **63**, 1195 (1989).
- [39] Widom, B. and Rowlinson, J.S., 1970, *J. Chem. Phys.*, **52**, 1670.
- [40] Goldstein, R.E. and Ashcroft, N.W., 1985, *Phys. Rev. Lett.*, **55**, 2164.
- [41] Keenan, J.H., Keyes, F.G., Hill, P.G. and Moore, J.G., 1992, *Steam Tables*, (Malabar: Krieger).
- [42] Grigull, U., Straub, J. and Schiebener, P., 1984, *Steam Tables in SI Units*, (Berlin, New York: Springer-Verlag).
- [43] Müller, E.A. and Gubbins, K.E., 1995, *I&EC Research*, **34**, 3662.

Table 1: Geometry and parameters for water models. The position of the negative charge (denoted M) for TIP4P/P, SCPDP and KJ is shifted from the position of oxygen atom (Lennard-Jones site) by  $r(\text{OM})$  toward the direction of the permanent dipole.  $\mathbf{m}_0$  is the permanent dipole moment and  $\alpha$  is the polarizability.

	TIP4P/P	SPC/P	SCPDP	KJ	TIP4P	SPC
$r(\text{OH})$ /nm	0.09572	0.1	0.1	0.0957	0.09572	0.1
$\angle \text{HOH}$ /deg	104.52	109.47	109.5	104.5	104.52	109.47
$\epsilon_{LJ}$ /kJ·mol <sup>-1</sup>	0.6490	0.6490	0.7696	1.7585	0.6490	0.6490
$\sigma_{LJ}$ /nm	0.3154	0.3167	0.3221	0.317	0.3154	0.3167
$Q_{\text{O}}$ /e		-0.6690		+1.2456		-0.82
$Q_{\text{H}}$ /e	+0.4418	+0.3345	+0.4049	+0.6228	+0.52	+0.41
$Q_{\text{M}}$ /e	-0.8836		-0.8098	-2.4912	-1.04	
$r(\text{OM})$ /nm	0.015		0.01	0.0138	0.015	
$\mathbf{m}_0$ /D	1.85	1.85	1.85	1.85	2.18	2.27
$\alpha$ /nm <sup>3</sup>	0.001444	0.001444	0.001444	0.00147	0	0

Table 2: Coexistence properties of polarizable water models.  $\rho$ ,  $u$ ,  $P_v$ , and  $\Delta H$  denote density, potential energy, vapor pressure, and heat of vaporization respectively. Subscripts indicate gas ( $g$ ) or liquid ( $l$ ) phase. For the TIP4P/P model, statistical errors in the last decimal point are shown in parentheses.

model	T/K	$\rho_g/\text{g}\cdot\text{cm}^{-3}$	$\rho_l/\text{g}\cdot\text{cm}^{-3}$	$u_g/\text{kJ}\cdot\text{mol}^{-1}$	$u_l/\text{kJ}\cdot\text{mol}^{-1}$	$P_v/\text{bar}$	$\Delta H/\text{kJ}\cdot\text{mol}^{-1}$
TIP4P/P	530	.049(1)	.811(3)	-3.4(1)	-29.3(1)	68(3)	28.2(2)
	540	.059(1)	.783(4)	-4.0(1)	-28.3(1)	84(3)	26.7(2)
	550	.073(1)	.738(8)	-4.7(0)	-26.9(2)	101(3)	24.4(2)
	560	.092(3)	.686(9)	-5.7(1)	-25.4(2)	122(3)	21.7(3)
	570	.119(6)	.632(7)	-7.0(0)	-23.8(1)	144(3)	18.6(4)
SPC/P	510	.056	.792	-3.5	-28.2	89	27.3
	520	.070	.756	-4.4	-24.0	107	25.1
	530	.091	.677	-5.6	-24.8	128	21.4
	540	.122	.600	-7.1	-22.8	152	17.4
SCPDP	480	.036	.758	-2.5	-28.1	45	27.7
	490	.045	.734	-3.1	-27.1	58	26.2
	500	.056	.691	-3.8	-25.6	73	24.0
	510	.070	.640	-4.7	-24.2	89	21.5
KJ	610	.054	.699	-3.7	-28.8	104	28.3
	620	.063	.685	-4.2	-28.1	120	27.1
	630	.073	.668	-4.7	-27.4	137	25.7
	640	.086	.645	-5.4	-26.4	156	23.8
	650	.104	.615	-6.3	-25.3	177	21.5
	660	.126	.578	-7.3	-24.0	199	18.9

Table 3: Estimates of critical temperature and density of polarizable water models. For the TIP4P/P model, statistical errors in the last decimal point are shown in parentheses. Experimental values are from reference [42].

model	$T_{cr}$ /K	$\rho_{cr}$ /g · cm <sup>-3</sup>
TIP4P/P	587(3)	0.35(2)
SPC/P	551	0.34
SCPDP	538	0.32
KJ	685	0.34
experiment	647	0.32

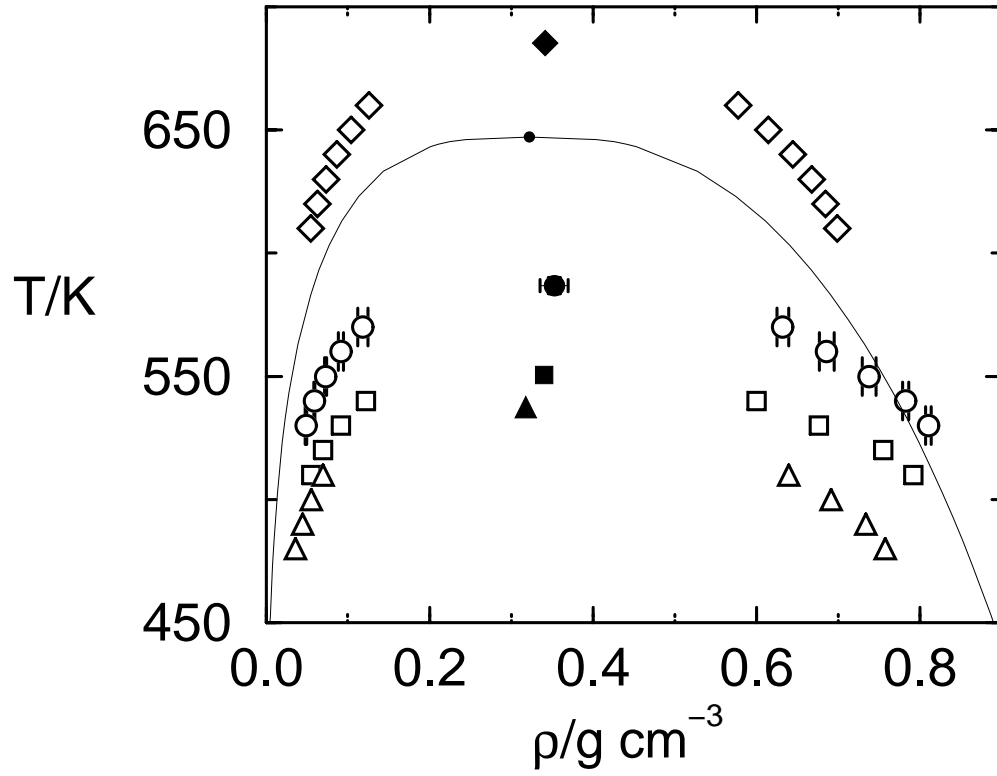


Figure 1: Coexistence density of polarizable water models. Circles are for the TIP4P/P model, squares are for the SPC/P model, triangles are for the SCPDP model, and diamonds are for the KJ model. The solid line is the experimental result [37]. Estimated critical points are shown as filled symbols. The statistical errors are shown for the TIP4P/P model.

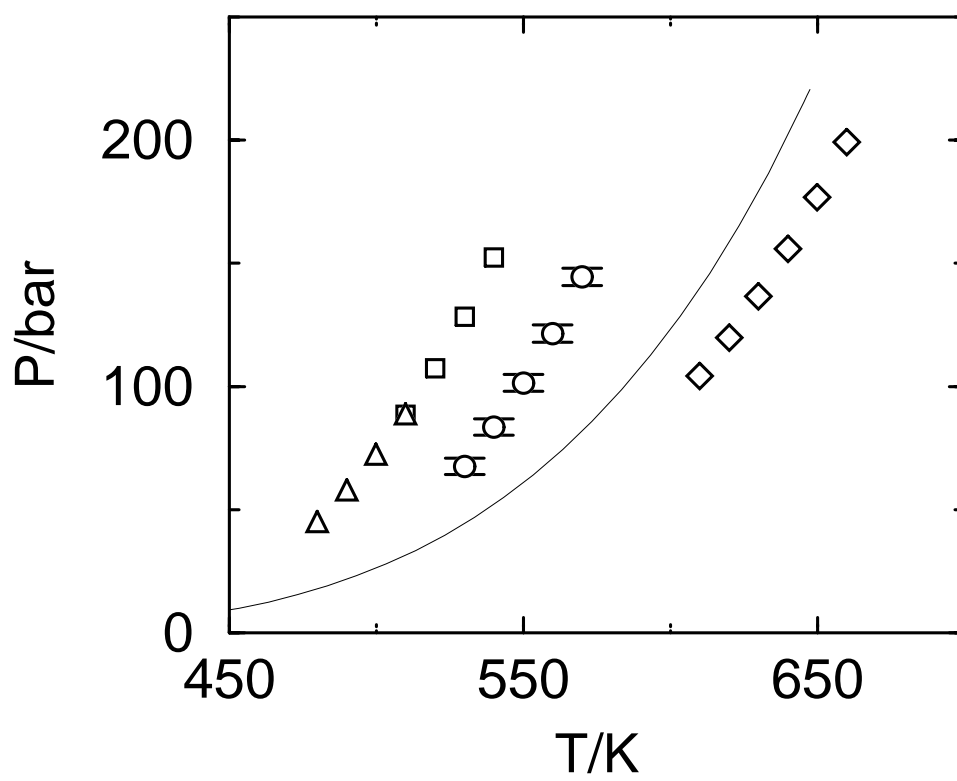


Figure 2: Vapor pressure of polarizable water models. Key as in figure 1.

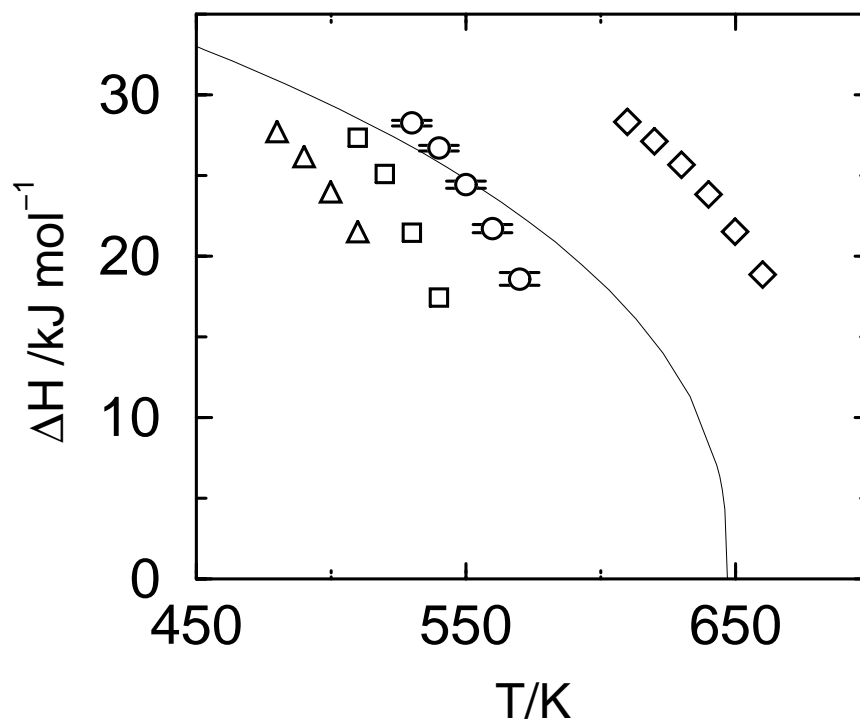


Figure 3: Heat of vaporization of polarizable water models. Key as in figure 1.

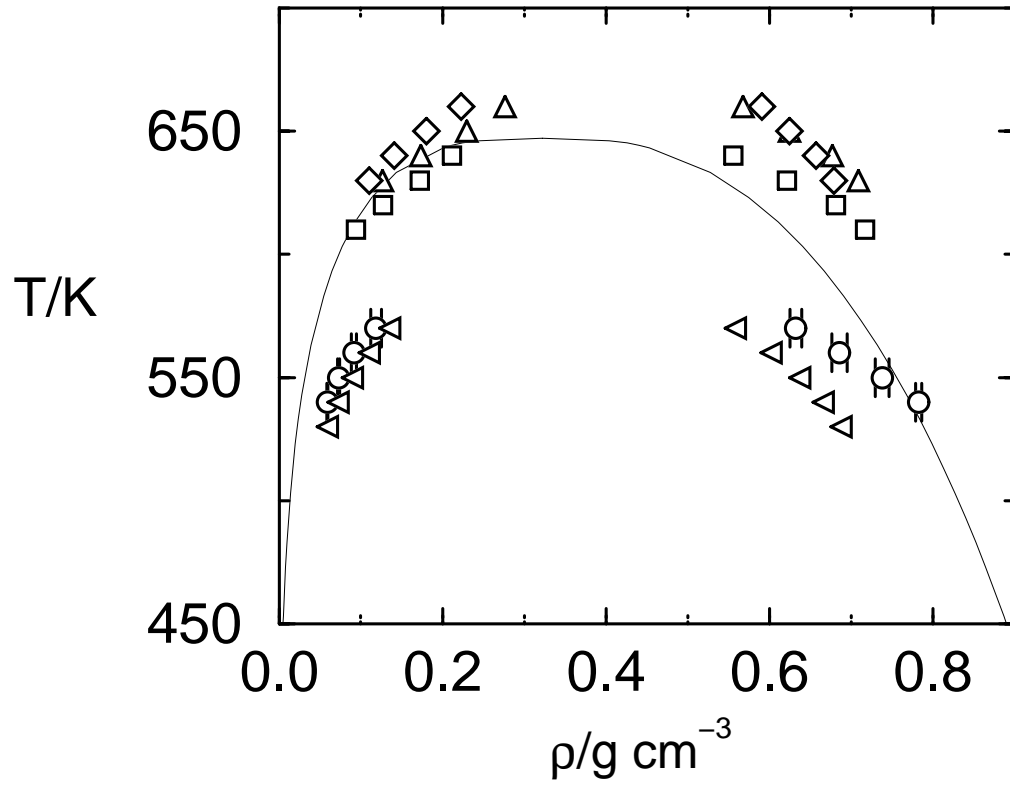


Figure 4: Coexistence density for variations of the TIP4P/P model. Squares,  $\sigma_{LJ}$  is reduced by 1%; upright-triangles,  $\epsilon_{LJ}$  was reduced by 20%; diamonds, the negative charge was shifted towards the positive charges on the H-O-H bisector by 0.005nm; left-triangles, the distance between the positive and negative charges was reduced by 1% from the original TIP4P/P model. The experimental results and the results of the original TIP4P/P are shown by the solid line and circles, respectively.